ISSN 2278-3091
Volume 8, No.5, September - October 2019
International Journal of Advanced Trends in Computer Science and Engineering
Available Online at http://www.warse.org/IJATCSE/static/pdf/file/ijatcse15852019.pdf
https://doi.org/10.30534/ijatcse/2019/15852019

Wireless Propagation Multipath Clustering: On Simultaneously Solving the Membership and the Number of Clusters

Jojo F. Blanza[1], Lawrence Materum[2]
[1, 2] Department of Electronics and Communications Engineering, De La Salle University, Manila, Philippines, jojo_f_blanza@dlsu.edu.ph
[1]Electronics Engineering Department, University of Santo Tomas, Manila, Philippines, jfblanza@ust.edu.ph

ABSTRACT

Multipaths from COST 2100 channel model (C2CM) semi-urban scenario obtained from IEEE DataPort are clustered using simultaneous clustering and model selection (SCAMS). SCAMS jointly solves the problem on model selection and clustering by determining simultaneously the number of clusters and their membership unlike well-known clustering approaches that give only the number of clusters. The number and membership of clusters depend on λ and γ, the parameters that weigh the penalty terms so that the trivial solution of the affinity matrix is avoided. The clustered multipaths from SCAMS are compared with the reference multipath clustering datasets available at IEEE DataPort using Jaccard index which examines the accuracy of the clustering approach.

Key words: channel models, clustering methods, data handling, data models, data preprocessing, multipath channels, radiowave propagation

1. INTRODUCTION

The European Cooperation in Science and Technology (COST) 2100 channel model can replicate the stochastic properties of multiple-input multiple-output (MIMO) propagation channels. C2CM is characterized by multipath clusters, groups of multipath components with similar delay and angles. A multipath component (MPC) is defined in delay and angular domains by its delay, angle of departure (Azimuth of Departure (AoD), Elevation of Departure (EoD)), and angle of arrival (Azimuth of Arrival (AoA), Elevation of Arrival (EoA)). Channel modeling is used to study the characteristics of wireless communications systems. The resulting model is very crucial for determining the performance of communications system. Many channel measurements and models indicate the clustering of multipaths. So the accuracy of channel models hinges on the accuracy of the clustering of multipaths. Most clustering approaches [1]–[5] give only the number of clusters as the accuracy measure. The problem with this is that eventhough the number of clusters is correct, there is no assurance that the membership of multipath clusters is accurate which would result in an inaccurate channel model. To solve the problem of determining the membership of the clusters, the study uses SCAMS to simultaneously solve the number of clusters and the membership of the clusters.

This study presents for the first time the results of SCAMS in clustering C2CM datasets in semi-urban scenarios taken from IEEE DataPort. It details the clustering of multipaths by simultaneously solving the number of clusters and their membership. The main contributions of this paper are (1) SCAMS is introduced to cluster multipaths in C2CM semi-urban scenarios; and (2) the results show that the clustering approach can be used as an alternative in the field of channel modeling.

The paper is organized in the following way. Section 2 describes the multipath datasets. Section 3 discusses the SCAMS clustering approach. Section 4 presents the results of SCAMS. Section 5 concludes the work.

2. MULTIPATH CLUSTERING DATASETS

A time-varying (denoted by t) channel impulse response is obtained by the superposition of MPCs from all the active multipath clusters based on the position of the MS. It is given in delay and direction domain as

$$h(t,\tau,\mathbf{\Psi}^{\mathrm{BS}},\mathbf{\Psi}^{\mathrm{MS}}) = \sum_{k=1}^{K}\sum_{p} a_{n,p}\delta(\tau-\tau_{n,p})\delta(\mathbf{\Psi}^{\mathrm{BS}}-\Psi_{n,p}^{\mathrm{BS}})\delta(\mathbf{\Psi}^{\mathrm{MS}}-\mathbf{\Psi}_{n,p}^{\mathrm{MS}}) \quad (1)$$

where K is the set of visible cluster indexes, $a_{n,p}$ is the complex amplitude of the pth MPC in the nth cluster, $\mathbf{\Psi}_{n,p}^{BS}$ is the direction of departure (AoD, EoD), and $\mathbf{\Psi}_{n,p}^{MS}$ is the direction of arrival (AoA, EoA) of the MPC. The overview of C2CM is presented in [6] while the specifics are discussed extensively in [7].

To have a common set of data that can be used in channel modeling, analyzing clustering approaches, and for purposes of comparing clustering accuracies, multipaths in indoor and semi-urban scenarios are taken from the multipath datasets in IEEE DataPort [8]. The details of the generation of the datasets can be found in [9]. The datasets used in this study as reference data in multipath clustering are the following:

1. Semi-Urban, B1, line-of-sight, single link
2. Semi-Urban, B2, line-of-sight, single link

There are thirty trials for each channel scenario with different number of multipaths and clusters. The power component in column 8 was not included in the clustering process. The cluster identifications or IDs in column 9 are not also included in the clustering process as they only serve as the reference IDs in comparing with the calculated IDs. The whitened data of columns 1 to 7 are normalized [0, 1] using

$$\boldsymbol{X}_{\text{normalized}} = (\boldsymbol{X}_{\text{whitened}} - \boldsymbol{X}_{\text{min}}) \circ (\boldsymbol{X}_{\text{max}} - \boldsymbol{X}_{\text{min}})^{-1} \quad (2)$$

where $\boldsymbol{X}_{\text{normalized}}$ is the normalized value of the whitened data, $\boldsymbol{X}_{\text{whitened}}$ is the whitened data in columns 1 to 7, $\boldsymbol{X}_{\text{max}}$ is the maximum data of each column, $\boldsymbol{X}_{\text{min}}$ is the minimum data of each column, and $\circ$ is the Hadamard product. Clustering results are greatly affected by the values of the affinities and (2) makes sure that the affinities are [0,1] for improved accuracy. The similarity between the computed data and the reference data is given by the Jaccard index η. The similarity measure is defined as

$$\eta = \frac{|\boldsymbol{C}_{\text{ref}} \cap \boldsymbol{C}_{\text{calc}}|}{|\boldsymbol{C}_{\text{ref}} \cup \boldsymbol{C}_{\text{calc}}|} = \frac{M_{11}}{M_{11}+M_{10}+M_{01}} \quad \in [0,1] \quad (3)$$

where $|\cdot|$ refers to cardinality, $\boldsymbol{C}_k \in \boldsymbol{C}$, $K = |\boldsymbol{C}|$ is the number of multipath clusters, $\boldsymbol{C}_{\text{ref}}$ is the reference clusters, $\boldsymbol{C}_{\text{calc}}$ is the calculated clusters, M_{11} is the total number of multipath clusters for the accuracy on the number of clusters or total number of multipaths for the accuracy on the membership of the clusters in $\boldsymbol{C}_{\text{ref}}$ that are the same as in $\boldsymbol{C}_{\text{calc}}$, M_{10} is the total number of multipath clusters for the accuracy on the number of clusters or total number of multipaths for the accuracy on the membership of the clusters in $\boldsymbol{C}_{\text{ref}}$ that are not in $\boldsymbol{C}_{\text{calc}}$, and M_{01} is the total number of multipath clusters for the accuracy on the number of clusters or total number of multipaths for the accuracy on the membership of the clusters in $\boldsymbol{C}_{\text{calc}}$ that are not in $\boldsymbol{C}_{\text{ref}}$.

3. SIMULTANEOUS CLUSTERING AND MODEL SELECTION (SCAMS)

The problem on clustering and estimating the number of clusters at the same time can be solved by SCAMS [10]–[11]. A given dataset $\boldsymbol{X}$ can be represented as $\boldsymbol{X}\boldsymbol{C}_{\text{calc}}$ where $\boldsymbol{C}_{\text{calc}}$ is generalized as an affinity matrix that can be formulated using the self-expression method [12]. The solution to

$$\min \|\boldsymbol{C}_{\text{calc}}\|_1 \quad \text{s.t.} \quad \boldsymbol{X} = \boldsymbol{X}\boldsymbol{C}_{\text{calc}}, \quad \text{diag}(\boldsymbol{C}_{\text{calc}}) = \boldsymbol{0} \quad (4)$$

corresponds to $\boldsymbol{C}_{\text{calc}}$. By denoting $\boldsymbol{W} = -\boldsymbol{C}_{\text{calc}}$ and introducing an ideal affinity matrix $\boldsymbol{C}_{\text{ideal}}$, the clustering problem can be expressed as

$$\begin{aligned} &\min \ \langle \boldsymbol{W}, \boldsymbol{C}_{\text{ideal}} \rangle, \\ &\text{s.t.} \ \boldsymbol{z}_k\{0,1\}^R, \quad \textstyle\sum_{k=1}^{K} \boldsymbol{z}_k = \boldsymbol{e}_M, \\ &\boldsymbol{C}_{\text{ideal}} = \textstyle\sum_{k=1}^{K} \boldsymbol{z}_k \circ \boldsymbol{z}_k, \qquad (\boldsymbol{C}_{\text{ideal}}) = K \end{aligned} \quad (5)$$

where $\langle \cdot,\cdot \rangle$ is the Frobenius inner product, $\boldsymbol{e}_M$ is an all one vector of size R. (5) can be expressed as an augmented Lagrange function

$$\begin{aligned} \boldsymbol{\mathcal{L}} = &\operatorname{tr}(\boldsymbol{W}^{\mathrm{T}}\boldsymbol{C}_{\text{ideal}}) + \lambda \operatorname{rank}(\boldsymbol{C}_{\text{ideal}}) + \gamma\|\boldsymbol{H}\|_0 + g(\boldsymbol{H}) \\ &+ \operatorname{tr}(\boldsymbol{Y}^{\mathrm{T}}(\boldsymbol{C}_{\text{ideal}} - \boldsymbol{H} + \operatorname{diag}(\boldsymbol{H}) - \boldsymbol{I})) \\ &+ \frac{1}{2\mu}\|\boldsymbol{C}_{\text{ideal}} - \boldsymbol{H} + \operatorname{diag}(\boldsymbol{H}) - \boldsymbol{I}\|_{\mathrm{F}}^2, \quad \text{s.t.} \ \boldsymbol{C}_{\text{ideal}} \in \boldsymbol{S}_+ \end{aligned} \quad (6)$$

where $\boldsymbol{H}$ is an intermediate variable introduced to make the problem tractable, g is the indicator function of the convex set $[0,1]^{R\times R}$, $\boldsymbol{Y}$ is the Lagrange parameter, $\boldsymbol{I}$ is an identity matrix, $\mu > 0$ is a penalty parameter, $\|\cdot\|_0$ is the ℓ_0 norm which counts the number of nonzero elements, λ and γ are the parameters to weigh the respective penalty terms, $\|\cdot\|_{\mathrm{F}}$ is the Frobenius norm, and $\mathbf{S}_+$ is the positive semi-definite cone. The Lagrange function can be minimized with respect to $\boldsymbol{C}_{\text{ideal}}$ and $\boldsymbol{H}$ alternatingly, by fixing the other variable, and then updating $\boldsymbol{Y}$. The overall framework of the Alternating Direction Method of Multipliers (ADMM) [13] which solves $\boldsymbol{C}_{\text{ideal}}$ is shown in Algorithm 1. $\boldsymbol{C}_{\text{ideal}}$ can be factorized as $\boldsymbol{Z}\boldsymbol{Z}^{\mathrm{T}}$ where $\boldsymbol{Z}$ is an indicator matrix whose rows indicate to which cluster a point belongs. $\boldsymbol{Z}$ can be solved by the Asso Constrained Boolean Matrix Factorization (AssoCBMF) [10] that is presented in Algorithm 2 where superscript $\boldsymbol{B}$ is a "Boolean" matrix containing only 0's and 1's, $|\cdot|$ is the cardinality of the Boolean matrix and defined as the number of 1's in it, $\oplus$ is the exclusive-or operation applied element-wise, $\boldsymbol{D}(i,j)$ is the association accuracy as for rule $\boldsymbol{C}_{\text{ideal}}{}^{\boldsymbol{B}}(j,:) \Rightarrow \boldsymbol{C}_{\text{ideal}}{}^{\boldsymbol{B}}(i,:)$, υ is a threshold for constructing $\boldsymbol{D}^{\boldsymbol{B}}$, and r_{thresh} is a threshold for deleting the j-th columns. The number of clusters and their membership are the output of the AssoCBMF algorithm.

Algorithm 1: Alternating Direction Method of Multipliers

Input: Negative affinity matrix $\boldsymbol{W}$, parameters λ and γ

Initialize: $\boldsymbol{C}_{\text{ideal}} = \boldsymbol{H} = \boldsymbol{Y} = \boldsymbol{0}_{N\times N}$, $\mu = 10^6$, $\rho = 1.1$, $\mu_{\min} = 10^{-10}$ and $\varepsilon = 10^{-8}$.

while not converged **do**

Step 1 Fix the others and update $\boldsymbol{C}_{\text{ideal}}$ as
$\boldsymbol{C}_{\text{ideal}} = \operatorname{argmin}_{\boldsymbol{C}_{\text{ideal}}} \|\boldsymbol{C}_{\text{ideal}} - \boldsymbol{H} + \mu(\boldsymbol{W} + \boldsymbol{Y})\|_{\mathrm{F}}^2 + 2\mu\lambda \operatorname{rank}(\boldsymbol{C}_{\text{ideal}}), \text{s.t.} \quad \boldsymbol{C}_{\text{ideal}} \in \mathbf{S}_+$.

Step 2 Fix the others and update $\boldsymbol{H}$ as
$\boldsymbol{H}' = \operatorname{argmin}_{\boldsymbol{H}} \|\boldsymbol{H} - \boldsymbol{C}_{\text{ideal}} - \mu\boldsymbol{Y}\|_{\mathrm{F}}^2 + 2\mu\gamma\|\boldsymbol{H}\|_0 + g(\boldsymbol{H})$,
$\boldsymbol{H} = \boldsymbol{H}' - \operatorname{diag}(\boldsymbol{H}') + \boldsymbol{I}$.

Step 3 Update the multipliers
$\mathbf{Y} = \mathbf{Y} + \frac{1}{\mu}(\boldsymbol{C}_{\text{ideal}} - \boldsymbol{H})$.

Step4 Update the parameter μ by
$\mu = \max\left(\frac{\mu}{\rho}, \mu_{\min}\right)$.

Step 5 Check the convergence conditions:
$\|\boldsymbol{C}_{\text{ideal}} - \boldsymbol{H}\|_\infty \leq \varepsilon$.

endwhile

(5)

4. RESULTS

By choosing the correct value of γ and using the calculated value of λ from [12], SCAMS gives the correct number of clusters. A value of γ that is less than or higher than the correct value leads to a lesser number or higher number of clusters than the correct number of clusters, respectively. Figure 1 shows the Jaccard index of the number of clusters in semi-urban B1 LOS single link versus the corresponding values of λ and γ. The minimum index is 0, the maximum index is 0.0455, and the mean index is 0.0186. Figure 2 presents the Jaccard index of the members per cluster in semi-urban B1. The minimum index is 0.1364 while the maximum index is 0.2452 with mean index of 0.1875. Figure 3 gives the Jaccard index of the number of clusters in semi-urban B2 LOS single link versus the corresponding values of λ and γ. The minimum index is 0, the maximum index is 0.0303, and the mean index is 0.0159. Figure 4 illustrates the Jaccard index of the members per cluster of semi-urban B2. The minimum index is 0.1420 while the maximum index is 0.2293 with mean index of 0.1818. Semi-urban B1 has twenty indices (in cyan) out of thirty above the mean for the number of clusters while fourteen indices (in cyan) out of thirty above the mean for the membership of the clusters. Semi-urban B2 has twenty indices (in cyan) out of thirty above the mean for the number of clusters while seventeen indices (in cyan) out of thirty above the mean for the membership of the clusters. SCAMS can be used as an alternative to cluster multipaths in semi-urban scenario but it gives lower accuracy compared to the results obtained in [14] for indoor scenario.

Algorithm 2: AssoConstrained Boolean Matrix Factorization

Input: $\boldsymbol{C}_{\text{ideal}}, K_0$

Initialize: Construct the Boolean matrix $\boldsymbol{C}_{\text{ideal}}{}^{\boldsymbol{B}}$ from $\boldsymbol{C}_{\text{ideal}}$ with rounding threshold $t_{\boldsymbol{B}} = 0.5, \boldsymbol{Z}^{\boldsymbol{B}} \leftarrow [\quad]$, $e = \infty, r_{\text{thresh}} = 0.1$.

for $\nu = 0.1, 0.2, \dots, 1$ **do**

Construct $\boldsymbol{D}^{\boldsymbol{B}}$ with $\boldsymbol{D}^{\boldsymbol{B}}(i,j) = \dfrac{\langle \boldsymbol{C}_{\text{ideal}}{}^{\boldsymbol{B}}(i,:), \boldsymbol{C}_{\text{ideal}}{}^{\boldsymbol{B}}(j,:)\rangle}{\langle \boldsymbol{C}_{\text{ideal}}{}^{\boldsymbol{B}}(j,:), \boldsymbol{C}_{\text{ideal}}{}^{\boldsymbol{B}}(j,:)\rangle} > \nu$.

for $k = 1, 2, \dots, K_0$ **do**

$i = \text{argmin}_i \left| \boldsymbol{C}_{\text{ideal}}{}^{\boldsymbol{B}} \oplus ([\boldsymbol{Z}^{\boldsymbol{B}}\boldsymbol{D}^{\boldsymbol{B}}(:,i)] \circ [\boldsymbol{Z}^{\boldsymbol{B}}\boldsymbol{D}^{\boldsymbol{B}}(:,i)]^{\mathrm{T}}) \right|$.

$\boldsymbol{Z}^{\boldsymbol{B}} \leftarrow [\boldsymbol{Z}^{\boldsymbol{B}}\boldsymbol{D}^{\boldsymbol{B}}(:,i)]$.

Delete all $j-$th columns with $\dfrac{\langle \boldsymbol{D}^{\boldsymbol{B}}(:,i), \boldsymbol{D}^{\boldsymbol{B}}(:,j)\rangle}{\|\boldsymbol{D}^{\boldsymbol{B}}(:,i)\|\|\boldsymbol{D}^{\boldsymbol{B}}(:,j)\|} > r_{\text{thresh}}$ from $\boldsymbol{D}^{\boldsymbol{B}}$

if $\boldsymbol{D}^{\boldsymbol{B}}$ is empty **or** $\min. \left| \boldsymbol{C}_{\text{ideal}}{}^{\boldsymbol{B}} \oplus (\boldsymbol{Z}^{\boldsymbol{B}} \circ \boldsymbol{Z}^{\boldsymbol{B}^{\mathrm{T}}}) \right|$,

s.t. $\boldsymbol{Z}^{\boldsymbol{B}^{\mathrm{T}}} \circ \boldsymbol{Z}^{\boldsymbol{B}} = \boldsymbol{I}_{K \times K}$ is not reduced in this loop

break

end if

if $\left\| \boldsymbol{C}_{\text{ideal}} - \boldsymbol{Z}^{\boldsymbol{B}}\boldsymbol{Z}^{\boldsymbol{B}^{\mathrm{T}}} \right\|_{\mathrm{F}}^2 < e$

$\boldsymbol{Z}^{\boldsymbol{B}^*} = \boldsymbol{Z}^{\boldsymbol{B}}$.

$e = \left\| \boldsymbol{C}_{\text{ideal}} - \boldsymbol{Z}^{\boldsymbol{B}}\boldsymbol{Z}^{\boldsymbol{B}^{\mathrm{T}}} \right\|_{\mathrm{F}}^2$.

end if

end for

end for

return $\boldsymbol{Z}^{\boldsymbol{B}^*}$

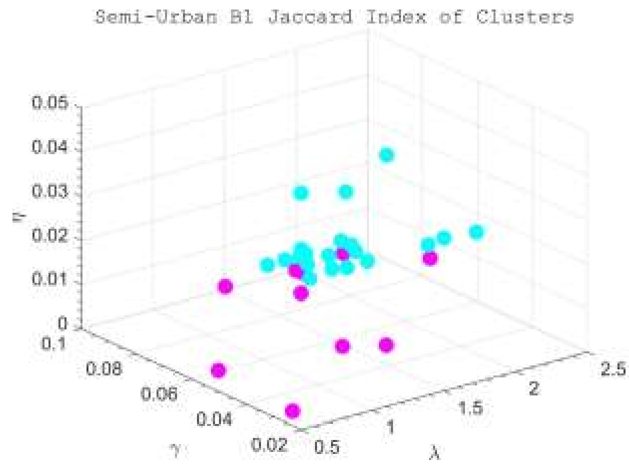

Figure 1: Jaccard index of clusters as a function of λ and γ in semi-urban B1 LOS single link where cyan colors are indices higher than the mean of 0.0186

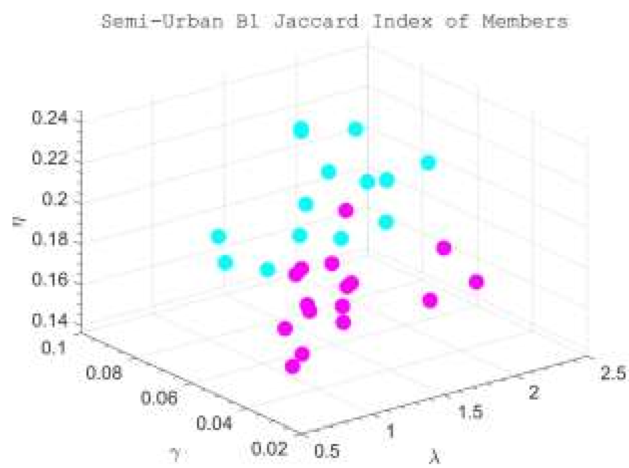

Figure 2: Jaccard index of members as a function of λ and γ in semi-urban B1 LOS single link where cyan colors are indices higher than the mean of 0.1875

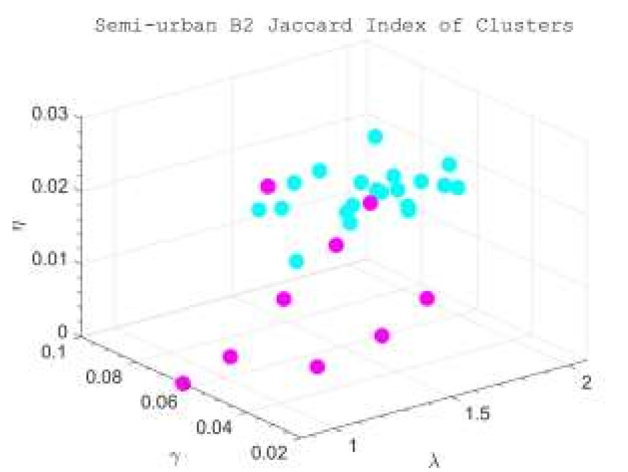

Figure 3: Jaccard index of clusters as a function of λ and γ in semi-urban B2 LOS single link where cyan colors are indices higher than the mean of 0.0159

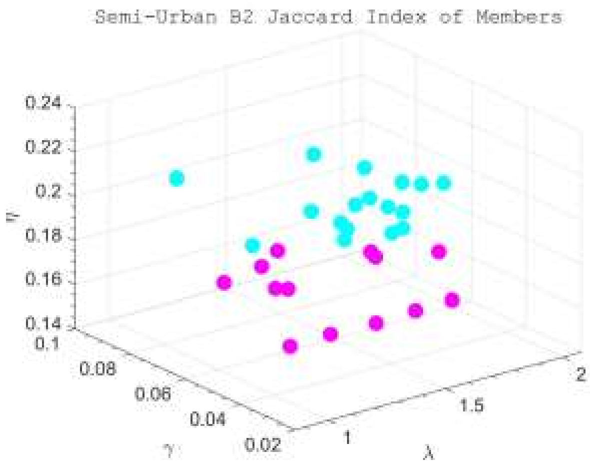

Figure 4: Jaccard index of members as a function of λ and γ in semi-urban B1 LOS single link where cyan colors are indices higher than the mean of 0.1818

Table 1: Jaccard Indices for the Number of Clusters of Semi-Urban LOS Single Link

	Jaccard Index	Relative Frequency
Semi-Urban B1	$\leq$ 0.1	100 %
Semi-Urban B2	$\leq$ 0.1	100 %

Table 2: Jaccard Indices for the Membership of Clusters of Semi-Urban LOS Single Link

	Jaccard Index	Relative Frequency
Semi-Urban B1	$\leq$ 0.2	70 %
	0.2 - 0.4	30 %
Semi-Urban B2	$\leq$ 0.2	80 %
	0.2 - 0.4	20 %

The relative frequency of the Jaccard indices for the number of clusters for both semi-urban B1 and B2 LOS single link is shown in Table 1 while that of the membership of the clusters for also both semi-urban B1 and B2 LOS single link is presented in Table 2. All of the indices have values less than 0.4 due to the wide angular spread of the multipaths and higher number of multipaths per cluster. Figure 5 displays a surface fit of the Jaccard index of the number of clusters in semi-urban B1 LOS single link as a function of λ and γ. The mathematical model generated is

$$\eta = -0.09334 + 0.2951\lambda - 1.232\gamma - 0.03053\lambda^2 - 8.077\lambda\gamma + 115.9\gamma^2 + 0.2169\lambda^2\gamma + 65.98\lambda\gamma^2 - 1215\gamma^3 \quad . \quad (7)$$

Figure 6 displays a surface fit of the Jaccard index of the membership of clusters in semi-urban B1 LOS single link as a function of λ and γ. The mathematical model generated is

$$\eta = 0.03656 + 0.2184\lambda + 2.112\gamma - 0.2489\lambda^2 + 9.439\lambda\gamma - 196.1\gamma^2 + 4.045\lambda^2\gamma - 214.6\lambda\gamma^2 + 3346\gamma^3 \quad . \quad (8)$$

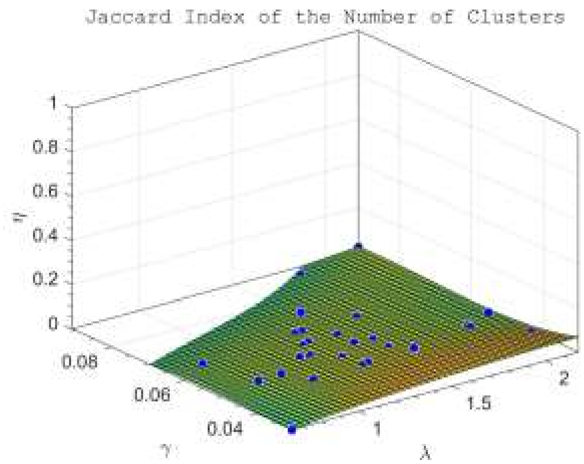

Figure 5: Curve fitting of Jaccard indices of the number of clusters for Semi-Urban B1 LOS Single link

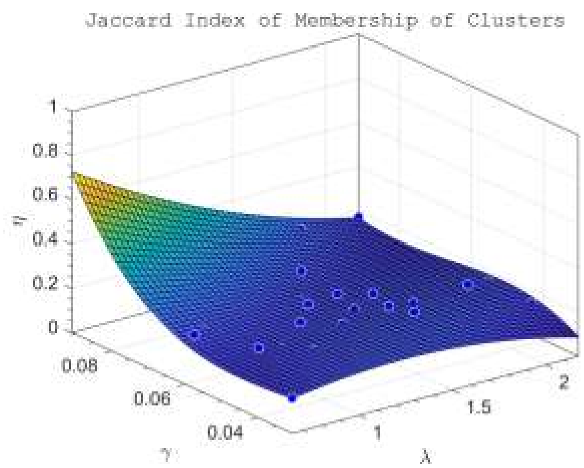

Figure 6: Curve fitting of Jaccard indices of the membership of clusters for Semi-Urban B1 LOS Single link

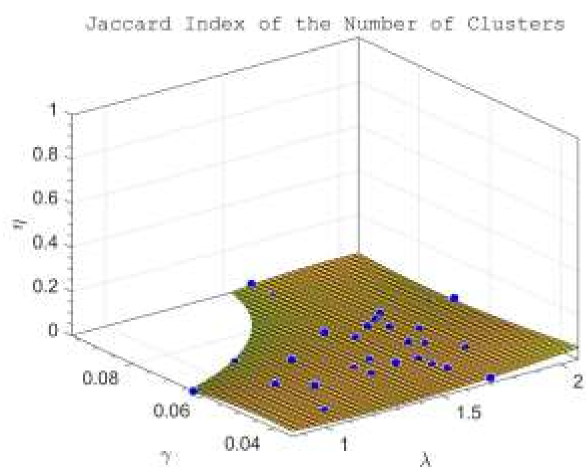

Figure 7: Curve fitting of Jaccard indices of the number of clusters for Semi-Urban B2 LOS Single link

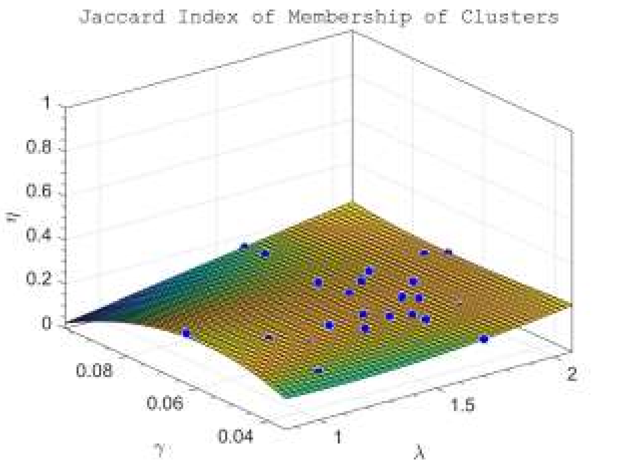

Figure 8: Curve fitting of Jaccard indices of the membership of clusters for Semi-Urban B2 LOS Single link

Figure 7 displays a surface fit of the Jaccard index of the number of clusters in semi-urban B2 LOS single link as a function of λ and γ. The mathematical model generated is

$$\eta = 0.06484 - 0.3335\lambda + 6.217\gamma + 0.1788\lambda^2 + 2.312\lambda\gamma - 134.6\gamma^2 - 3.204\lambda^2\gamma + 66.57\lambda\gamma^2 + 127.2\gamma^3 . \quad (9)$$

Figure 8 displays a surface fit of the Jaccard index of the membership of clusters in semi-urban B2 LOS single link as a function of λ and γ. The mathematical model generated is

$$\eta = -0.4781 + 0.08024\lambda + 30.55\gamma + 0.1233\lambda^2 - 11.59\lambda\gamma - 311.2\gamma^2 - 1.295\lambda^2\gamma + 128.7\lambda\gamma^2 + 359.7\gamma^3 . \quad (10)$$

All of the coefficients of the mathematical models have 95% confidence bounds. The value of the Jaccard index can be calculated by specifying the values of λ and γ.

5. CONCLUSION

This paper presents the results of SCAMS in clustering multipaths. SCAMS determines simultaneously the number of clusters and their membership which are dependent on λ and γ. The reference data were taken from C2CM semi-urban B1 and B2 LOS single link obtained from the IEEE DataPort. The whitened data were first normalized to give positive values of the affinities which can enhance the outcome of the clustering process. Results show that SCAMS can be used as an alternative to cluster multipaths and that the clustering approach can still be improved for its accuracy performance to get better. In particular, the selection and values of λ and γ parameters of SCAMS need to be done well or modified in their formulations. The results point to better alternatives, but also the necessity of performing concurrent determination of the membership of multipath and the number of multipath clusters.

ACKNOWLEDGEMENT

The authors would like to thank the Department of Science and Technology-Engineering Research and Development for Technology (DOST-ERDT) and De La Salle University for financial support.

REFERENCES

1. N. Czink, P. Cera, J. Salo, E. Bonek, J.-P. Nuutinen, and J. Ylitalo. **A framework for automatic clustering of parametric MIMO channel data including path powers**, in *IEEE 64th Veh. Technol. Conf.*, pp. 1–5, 2006. https://doi.org/10.1109/VTCF.2006.35
2. C. Gentile. **Using the kurtosis measure to identify clusters in wireless channel impulse responses**, *IEEE Trans. Antennas Propag.*, vol. 61, no. 6, pp. 3392-3395, 2013. https://doi.org/10.1109/TAP.2013.2253299
3. R. He, Q. Li, B. Ai, Y. Geng, A. Molisch, V. Kristem, Z. Zhong, and J. Yu. **A kernel-power-density-based algorithm for channel multipath components clustering**, *IEEE Trans. Wireless Commun.*, vol. 16, no. 11, pp. 7138-7151, 2017. https://doi.org/10.1109/TWC.2017.2740206
4. Y. Li, J. Zhang, Z. Ma, and Y. Zhang. **Clustering analysis in the wireless propagation channel with a variational Gaussian mixture model**, *IEEE Trans. Big Data*, 2018.
5. A. Teologo and L. Materum. **Cluster-Wise Jaccard Accuracy of KPower Means on Multipath Datasets**, *Int. J. Adv. Trends Comput. Sci. Eng.*, *Int. J. Emerg. Trends Eng. Res.*, vol. 7, no. 8, pp. 203-208, 2019. https://doi.org/10.30534/ijeter/2019/16782019
6. L. Liu, C. Oestges, J. Poutanen, K. Haneda, P. Vainikainen, F. Quitin, F. Tufvesson, and P. De Doncker. **The COST 2100 MIMO channel**, *IEEE Trans. Wireless Commun.*, vol. 19, no. 6, pp. 92-99, 2012. https://doi.org/10.1109/MWC.2012.6393523
7. R. Verdone and A. Zanella. **Pervasive Mobile and Ambient Wireless Communications: COST Action 2100**, Springer Science & Business Media, 2012, ch. 3. https://doi.org/10.1007/978-1-4471-2315-6
8. J. Blanza, A. Teologo, and L. Materum. **Datasets for multipath clustering at 285 MHz and 5.3 GHz bands based on COST 2100 MIMO channel model**, [Online]. Available: http://dx.doi.org/10.21227/4cb9-hf81, 2019.
9. J. Blanza, A. Teologo, and L. Materum. **Datasets for multipath clustering at 285 MHz and 5.3 GHz bands based on COST 2100 MIMO channel model**, accepted in *9th Int. Symp. Multimedia Commun.*, Aug. 2019.
10. Z. Li, L. Cheong, and S. Zhou. **SCAMS: Simultaneous clustering and model selection**, in *Proc. IEEE Conf. Comput. Vision Pattern Recognit.*, pp. 264-271, 2014.
11. Z. Li, L. Cheong, S. Yang, and K. Toh. **Simultaneous clustering and model selection: Algorithm, theory and applications**, *IEEE Trans. Pattern Anal. Mach. Intell.*, vol. 40, no. 8, pp. 1964–1978, 2018. https://doi.org/10.1109/TPAMI.2017.2739147
12. E. Elhamifar and R. Vidal. **Sparse subspace clustering: Algorithm, theory, and applications**, *IEEE Trans.*

Pattern Anal. Mach. Intell., vol. 35, no. 11, pp. 2765-2781, 2013.
https://doi.org/10.1109/TPAMI.2013.57

13. S. Boyd, N. Parikh, E. Chu, B. Peleato, J. Eckstein, et al. **Distributed optimization and statistical learning via the alternating direction method of multipliers**, *Found. Trends Mach. Learn.*, 3(1):1–122, 2011.
https://doi.org/10.1561/2200000016
14. J. Blanza and L. Materum. **Grouping of COST 2100 indoor multipaths using simultaneous clustering and model selection**, *Int. J. Emerg. Trends Eng. Res.*, vol. 7, no. 8, pp. 197-202, 2019.
https://doi.org/10.30534/ijeter/2019/15782019